Published in final edited form as:
Biochemistry. 2013 June 11; 52(23): 4075–4088. doi:10.1021/bi4004952.

Kinetics of O^6-Pyridyloxobutyl-2′-deoxyguanosine Repair by Human O^6-alkylguanine DNA Alkyltransferase

Delshanee Kotandeniya[†], **Daniel Murphy**[†], **Shuo Yan**[†], **Soobong Park**[†], **Uthpala Seneviratne**[†], **Joseph S. Koopmeiners**[£], **Anthony Pegg**[€], **Sreenivas Kanugula**[€], **Fekadu Kassie**[¥], and **Natalia Tretyakova**[†,*]

[†]Department of Medicinal Chemistry and the Masonic Cancer Center, University of Minnesota, Minneapolis, Minnesota 55455

[£]Division of Biostatistics, University of Minnesota, Minneapolis, Minnesota 55455

[€]Department of Cellular and Molecular Physiology, Pennsylvania State University College of Medicine, Hershey, Pennsylvania 17033

[¥]Department of Veterinary Clinical Sciences, College of Veterinary Medicine, and Masonic Cancer Center

Abstract

Tobacco-specific nitrosamines 4-(methylnitrosamino)-1-(3-pyridyl)-1-butanone (NNK) and N-nitrosonicotine (NNN) are potent carcinogens believed to contribute to the development of lung tumors in smokers. NNK and NNN are metabolized to DNA-reactive species that form a range of nucleobase adducts, including bulky O^6-[4-oxo-4-(3-pyridyl)but-1-yl]deoxyguanosine (O^6-POB-dG) lesions. If not repaired, O^6-POB-dG adducts induce large numbers of G → A and G → T mutations. Previous studies have shown that O^6-POB-dG can be directly repaired by O^6-alkylguanine-DNA alkyltransferase (AGT), which transfers the pyridyloxobutyl group from O^6-alkylguanines in DNA to an active site cysteine residue within the protein. In the present study, we investigated the influence of DNA sequence context and endogenous cytosine methylation on the kinetics of AGT-dependent repair of O^6-POB-dG in duplex DNA. Synthetic oligodeoxynucleotide duplexes containing site-specific O^6-POB-dG adducts within *K-ras* and *p53* gene-derived DNA sequences were incubated with recombinant human AGT protein, and the kinetics of POB group transfer was monitored by isotope dilution HPLC-ESI$^+$-MS/MS analysis of O^6-POB-dG remaining in DNA over time. We found that the second order rates of AGT-mediated repair were influenced by DNA sequence context (10-fold differences), but were only weakly affected by the methylation status of neighboring cytosines. Overall, AGT-mediated repair of O^6-POB-dG was 2–7 times slower than that of O^6-Me-dG adducts. To evaluate the contribution of AGT to O^6-POB-dG repair in human lung, normal human bronchial epithelial cells (HBEC) were treated with model pyridyloxobutylating agent, and O^6-POB-dG adduct repair over time was monitored by HPLC-ESI$^+$-MS/MS. We found that HBEC cells were capable of removing O^6-POB-dG lesions, and the repair rates were significantly reduced in the presence of AGT inhibitor (O^6-benzylguanine). Taken together, our results suggest that AGT plays an important role in protecting human lung against tobacco nitrosamine-mediated DNA damage and that inefficient AGT repair

*Corresponding author: 760 MCRB, Masonic Cancer Center, University of Minnesota, 420 Delaware St. SE - MMC 806, Minneapolis, Minnesota 55455; Tel.: 612-626-3432; Fax: 612-626-5135; trety001@umn.edu.

Supporting Information

Supporting information includes DNA melting curves (S-1), results of statistical analyses (Tables S-2, S-3 and S-4), cytotoxicity data for HBEC cells treated with NNKOAC (S-5), a sample HPLC-UV trace showing purity of *(−) K-ras*-POB oligonucleotide strand (S-6) and HPLC ESI$^-$ MS spectra for the synthetic oligodeoxynucleotides used in this work (S-7). This material is available free of charge via the Internet at http://pubs.acs.org.

of O^6-POB-dG at specific sequence contributes to mutational spectra observed in smoking-induced lung cancer.

Introduction

Nicotine-derived nitrosamines NNK (4-(methylnitrosamino)-1-(3-pyridyl)-1-butanone) and NNN (N-nitrosonicotine)[1] are among the most potent lung carcinogens present in cigarette smoke. Cytochrome P450-mediated hydroxylation of the α-methylene position of NNK produces methyl diazonium ions, while hydroxylation of the methyl group of NNK generates pyridyloxobutyl diazonium ions (Scheme 1).[2–5] Pyridyloxobutyl diazonium ions are also formed upon metabolic activation of NNN.[2,6] Methyl diazonium and pyridyloxobutyl diazonium ions are strongly electrophilic species that modify multiple positions of DNA to give a range of nucleobase adducts, including N7-methyl-deoxyguanosine (N7-Me-dG), O^6-methyl-deoxyguanosine (O^6-Me-dG), N7-[4-oxo-4-(3-pyridyl)-but-1-yl]deoxyguanosine (N7-POB-dG), O^6-[4-oxo-4-(3-pyridyl)but-1-yl]deoxyguanosine (O^6-POB-dG), O^2-[4-(3-pyridyl)-4-oxobut-1-yl]thymidine (O^2-POB-T), O^2-[4-(3-pyridyl)-4-oxobut-1-yl]-deoxycytidine (O^2-POB-dC), and O^4-methyl-deoxythymidine (O^4-Me-dT).[7] Among these, O^6-methyl-deoxyguanosine (O^6-Me-dG) and O^6-pyridyloxobutyl-deoxyguanosine (O^6-POB-dG) (Scheme 1) are known to be strongly miscoding lesions that are thought to contribute to NNK-mediated lung tumor formation in A/J mice.[6,8–11]

O^6-alkylguanine-DNA alkyltransferase (AGT) protein can directly remove the O^6-alkyl group from O^6-alkylguanines in DNA, restoring normal guanine (Scheme 2).[12–14] AGT protein binds to the minor groove of DNA via the helix-turn-helix motif, inducing flipping of O^6-Alk-dG out of the DNA helix to enter the protein active site.[12,15,16] Cysteine-145 thiol within the active site of the AGT protein is deprotonated via interactions with other active site residues, and the resulting Cys-145 thiolate anion undergoes nucleophilic attack at the α-carbon of the O^6-alkyl group, leading to its transfer from DNA to the protein (Scheme 2).[12,15] Alkylation of Cys145 inactivates the AGT protein and destabilizes its structure, signaling for protein ubiquitination and proteasomal degradation.[17,18] Since the protein is not regenerated following repair reaction, AGT acts non-enzymatically but rather as a stoichiometric reactant, with one molecule of protein used up per each adduct repaired.[14] Recent studies suggest that AGT binds DNA to form cooperative clusters; this cooperative DNA binding appears to be important for lesion search and/or repair.[19,20]

Previous studies by several laboratories, including ours, have revealed that the efficiency of AGT-mediated repair of O^6-alkylguanine adducts can be influenced by the local DNA sequence context.[21,22] For example, the Spratt laboratory employed first order kinetics[23] to examine the rates of repair of alkylguanine lesions placed within *H-ras* codon 12 (G_1G_2A).[21] The relative rates of AGT-mediated alkyl transfer were dependent on the alkyl group identity, e.g. benzyl > methyl > ethyl > 2-hydroxyethyl > 4-(3-pyridyl)-4-oxobutyl (POB), and dealkylation rates were greater for adducts present at G_1 as compared to those on G_2.[21] It has been suggested that in some sequence contexts, bulky alkylguanine lesions may bind to the AGT protein in an inactive conformation that is not conductive to alkyl transfer.[21] However, the published kinetic data for O^6-POB-dG adduct repair is limited to *H-ras* codon 12, while other DNA sequences have not been previously examined.

AGT repair rates can also be affected by neighboring 5-methylcytosine (^{Me}C), an epigenetic nucleobase modification that is present at all CpG dinuclotides within the coding sequence of the human *p53* tumor suppressor gene.[24] The majority of *p53* mutations associated with smoking are found at guanine bases within endogenously methylated ^{Me}CpG dinucleotides, e.g. codons 157, 158, 245, 248, and 273. [25–28] One possible mechanism for the increased

mutagenesis at these sites involves inefficient repair of tobacco carcinogen-induced DNA adducts such as O^6-Me-dG and O^6-POB-dG, leading to their accumulation at methylated CpG sequences. Indeed, inactivation of the AGT gene by hypermethylation of the promoter region results in a significant increase in G → A *p53* gene mutations in non-small cell lung cancer.[29] Our earlier study has demonstrated that AGT binding and repair of O^6-Me-dG was only weakly affected by C-5 methylation of neighboring cytosine bases.[30] However, similar experiments have not been conducted for O^6-POB-dG.

In the present study, we employed a mass spectrometry-based methodology developed in our laboratory[31] to investigate AGT repair of O^6-POB-dG adducts placed within the context of the *K-ras* gene (5′-G_1TA G_2TT G_3G_4A G_5CT G_6G_7T G_8G_9C G_{10}T-3′, where G3, G4, G5, G6, or G7 = O^6-POB-dG). We also examined the influence of cytosine methylation on AGT-mediated repair of O^6-POB-dG adduct present within frequently mutated *p53* codons 157, 158, 245, 248, 249, and 273.[32] Finally, we evaluated the kinetics of O^6-POB-dG repair in human bronchial epithelial cells (HBEC) in the absence and in the presence of AGT inhibitor.

Experimental Procedures

Materials

1,3-Dithiane protected O^6-POB-dG (O^6-[3-[2-(3-pyridyl)-1,3-dithyan-2-yl]propyl]-deoxyguanosine) was synthesized according to a previously published method[33] and converted to its corresponding phosphoramidite using standard phosphoramidite chemistry.[34] Standard nucleoside phosphoramidites, solvents, and solid supports for the solid phase synthesis of oligodeoxynucleotides were purchased from Glen Research Corporation (Sterling, VA). γ-^{32}P-ATP was obtained from Perkin Elmer Life Sciences (Waltham, MA), while T4-PNK enzyme and buffer were procured from New England Biolabs (Ipswich, MA). MicroSpin Illustra G25 columns were obtained from GE Healthcare (Buckinghamshire, UK). 29% Acrylamide solution was purchased from BioRad (Hercules, CA). Tetramethylethylenediamine (TEMED) and ammonium persulfate were obtained from Sigma-Aldrich (Milwaukee, WI). 4-(Acetoxymethylnitrosamino)-1-(3-pyridyl)-1-butanone (NNKOAc) was purchased from Toronto research Chemicals (Toronto, Canada). The rest of the chemicals employed in the study were from Sigma-Aldrich (Milwaukee, WI) or Fisher Scientific (Fairlawn, NJ). Human recombinant AGT protein with a C-terminal histidine tail (WT hAGT) and its C145A variant were expressed in *E. coli* and isolated as reported elsewhere.[35,36] The activity of the AGT protein was determined by titrating the recombinant protein with DNA duplexes containing site specific O^6-MeG, followed by HPLC-ESI$^+$-MS/MS analysis as described previously.[31,37] D_4-O^6-POB-dG was a gift from Professor Stephen Hecht (University of Minnesota Masonic Cancer Center). HBEC cells were grown in Keratinocyte SFM media (Life Technologies, NY) supplemented with human recombinant Epidermal Growth Factor (EGF 1-53, Life Technologies, NY) and Bovine Pituitary Extract media (Life Technologies, NY).

Preparation of O^6-POB-dG containing DNA

Synthetic oligodeoxynucleotides containing O^6-POB-dG adducts within the context of *K-ras* and *p53* genes were prepared by solid phase DNA synthesis using 5′-O-(4,4′-dimethoxytrityl)-*N,N*-dimethyl-formamidine-O^6-{3-[2-(3-pyridyl)-1,3-dithyan-2-yl]propyl}-2′-deoxyguanosine-3′-[(2-cyanoethyl)-(*N,N*-diisopropyl)]-phosphoramidite synthesized as described elsewhere.[34] The oligonucleotides were cleaved from the solid support and deprotected using concentrated ammonia (55 °C, 18 h) and dried, followed by deprotection of the dithiane group with 10 equivalents of fresh 10mg/ml *N*-chlorosuccinimide solution in 80% acetonitrile (30 min at room temperature in the dark).[34]

Synthetic oligodeoxynucleotides were purified by reverse phase HPLC using an Agilent 1100 HPLC system and a Supelcosil LC-18DB column (10 mm × 250 mm, 5 μm) maintained at 40 °C. HPLC solvents were 100 mM TEAAc (Buffer A, pH 7) and acetonitrile containing 50% A (Buffer B). A linear gradient of 16.8% to 26% B in 21 min and further to 38% B over the next 14 min was used.[37–39] All oligodeoxynucleotides used in this work were of > 99% purity (see HPLC traces in Supporting Information, S-6). The molecular weights of all synthetic DNA oligomers were confirmed by capillary HPLC-ESI$^-$ MS (Table 1), and their concentrations were determined by dG quantitation in enzymatic digests.[40]

To prepare double stranded DNA substrates for repair experiments, complementary DNA strands (6 nmol each) were combined in 10 mM Tris-HCl buffer (pH 8) containing 50 mM NaCl (30 μl). The mixture was heated at 90 °C for 5 minutes and slowly cooled to room temperature to produce double stranded DNA.[38]

Determination of DNA Melting Temperatures

DNA duplexes containing site specific O^6-POB-dG adducts (3 nmol) were dissolved in sodium phosphate buffer (10 mM, pH 7.0) containing 50 mM sodium chloride (9.7 μM DNA). DNA melting temperatures were obtained with a Varian Cary-100 Bio UV-visible spectrophotometer using a temperature gradient between 30 and 90 °C. Temperature increments or decrements of 0.5 °C/min were used. The experiment was repeated 4–6 times to determine DNA melting temperatures using Cary WinUV Thermal software (Varian, Palo Alto, CA) (Table 2).

Single Time Point AGT Repair Experiments

DNA duplexes containing O^6-POB-G at a specified site (500 fmol) were mixed with recombinant human AGT protein (400 fmol) in 50 mM Tris-HCl buffer (pH 7.8) containing 0.1 mM EDTA, 0.5 mg/mL BSA, and 0.5 mM DTT (final volume, 90 μl) and incubated at room temperature for 15 s. The repair reactions were quenched with 0.1N HCl, fortified with D_4-O^6-POB-dG (500 fmol, internal standard for mass spectrometry), and subjected to acidic hydrolysis (70 °C, 1 h) to release O^6-POB-G and D_4-O^6-POB-G. The reaction mixtures were neutralized with NH_4OH. O^6-POB-G and D_4- O^6-POB-G were purified by solid phase extraction (SPE) on Strata X cartridges.[31] O^6-POB-G was quantified by capillary HPLC-ESI$^+$-MS/MS using D_4- O^6-POB-G internal standard as described elsewhere.[31] Data reported are an average of 9–14 individual experiments.

Time Course AGT Repair Experiments

Human recombinant AGT protein (400 fmol) was combined with O^6-POB-dG-containing DNA duplexes (500 fmol) in 50 mM Tris-HCl buffer (pH 7.8) containing 0.1 mM EDTA, 0.5 mg/mL BSA, and 0.5 mM DTT (final volume, 90 μl). The resulting mixtures were incubated at room temperature for specified time periods (0–50 seconds) and manually quenched with 0.2 N HCl (90 μl, 0.1N final concentration). Following the addition of D_4-O^6-POB-dG internal standard (250 fmol), the DNA was hydrolyzed by heating at 70 °C for 1 h and neutralized with 0.2 N ammonium hydroxide. O^6-POB-G and D_4- O^6-POB-G were purified by solid phase extraction (SPE) and quantified by capillary HPLC-ESI$^+$-MS/MS as described previously.[31]

The concentrations of O^6-POB-G repaired at time t were plotted as a function of time, and the resulting data were fitted to the 2nd order kinetic equation (Equation 1)[30] using the KaleidaGraph software program (Synergy Software, Reading, PA):

$$kt = \frac{1}{B_0 - A_0} x \ln \frac{A_0(B_0 - C_t)}{B_0(A_0 - C_t)} \quad (1)$$

where A_0 is the concentration of AGT protein used, B_0 is the initial concentration of O^6-POB-dG containing DNA, C_t is the concentration of O^6-POB-G repaired at time t, and k is the 2nd order rate of O^6-POB-G repair.

Electrophoretic Mobility (Gel Shift) Assay

Elecrophoretic mobility (gel shift) experiments were conducted according to the previously published protocols.[30,41] In brief, O^6-POB-dG- containing double stranded DNA was end-labeled in the presence of γ-^{32}P-ATP and polynucleotide kinase. Excess γ-^{32}P-ATP was removed with MicroSpin Illustra G25 columns (GE Healthcare). The resulting 5′-^{32}P-end-labeled DNA duplexes (2 pmol, 0.1 μM) were spiked with the corresponding unlabeled DNA (0.8 μM) and calf thymus (CT) DNA (1 μg) and dissolved in 50 mM Tris-HCl, pH 7.8, buffer containing 0.1 mM EDTA, 0.5 mM DTT, and 0.5 mg/ml BSA. Human recombinant C145A AGT protein was added (0–6 μM), and the solutions were incubated at room temperature for 45 min. DNA-protein complexes were detected using 10% PAGE (acrylamide:N,N′-methylene bisacrylamide = 29:1 cast in 100 mM TAE buffer, pH 7.6). The gels were run in 10 mM Tris-acetate buffer (pH 7.6) at 100 V for 2.5 hours and imaged using a Molecular Dynamics STORM 840 phosphorimager (Amersham Biosciences Corporation, Piscataway, NJ). The radiolabeled DNA bands were quantified by densitometry using the ImageQuant software. Dissociation constants (K_d) were determined by plotting the $[D]/[D]_T$ ratios vs. $[P]_T$, where [D], $[D]_T$ and $[P]_T$ are the molar concentrations of free DNA, total DNA, and AGT protein, respectively. The data were fitted to the equation 2: [30,42]

$$\frac{[D]}{[D]_T} = \frac{K_d}{K_d + [P]_T} \quad (2)$$

The values of [D] and $[D]_T$ were calculated from the density of radioactive bands on the gel.

Cell Cytotoxicity Assays used to determine the Concentration of NNKOAC to use in the O^6-POB-G repair

Human bronchial epithelial cells (HBEC, 5×10^3) were seeded into a 96 well plate and allowed to grow overnight in 150 μl of Keratinocyte SFM media (Life Technologies, NY) supplemented with human recombinant Epidermal Growth Factor (EGF 1-53) and Bovine Pituitary Extract (37 °C, 5% CO_2). Cells (in triplicate) were treated with 0 – 400 μM NNKOAC for 1 h at 37 °C and 5% CO_2. Following treatment, carcinogen-containing media was removed, and the cells were washed with PBS buffer and allowed to grow in Keratinocyte SFM media (150 μl) for 48 h. To determine cell viability, they were treated with MTT reagent (37 °C, 5% CO_2, 2 h), followed by cell density measurements with a Biotek LLX808 microplate reader (BioTek, VT).

O^6-POB-G Adduct Formation and Repair in Human Bronchial Epithelial Cells (HBEC)

Human Bronchial Epithelial Cells (HBEC) were grown in Keratinocyte SFM media (Life Technologies, NY) supplemented with human recombinant Epidermal Growth Factor (EGF 1-53) and Bovine Pituitary Extract (37 °C, 5% CO_2) until fully confluent. Cells (in triplicate, 15 cm dishes) were treated with 150 μM NNKOAc or DMSO control for 1 h. Following treatment, carcinogen-containing media was removed, and the cells were washed three times with PBS buffer (Life Technologies, NY). Following the addition of normal growth media,

cells were incubated at 37 °C in 5% CO_2 for specified periods of time (0, 1, 2, 4, 8 and 12 h) to allow for adduct repair. At the end of incubation, the cells were washed, harvested, and stored at −80 °C until DNA extraction.

For experiments including AGT inhibitor (O^6-Bz-G), fully confluent HBEC cells were pre-treated with 10 μM O^6-Bz-G for 10 min (37 °C, 5% CO_2), followed by 150 μM NNKOAc/ 10 μM O^6-Bz-G treatment for 1 h at 37 °C under 5% CO_2 atmosphere as described above. Control cells were treated with O^6-Bz-G only. Carcinogen-containing media was replaced with fresh media containing 5 μM O^6-Bz-G, and the cells were incubated at 37 °C in 5% CO_2 for the specified lengths of time (0, 1, 2, 4, 8, or 12 h). At the end of the repair period, the cells were washed, harvested, and stored at − 80 °C until DNA extraction.

DNA Isolation from HBEC Cells

NNKOAc-treated HBEC cells ($4 – 4.5 \times 10^6$) were lysed with 2X cell lysis buffer (20 mM Tris HCl (pH 7.5), 10 mM $MgCl_2$, 2% (v/v) Triton-X, 650 mM sucrose, 30 min on ice) and pelleted at 4000 rpm for 15 min. The nuclei were suspended in 0.5 ml saline-EDTA solution (75 mM NaCl, 24 mM EDTA, pH 8) and digested with RNase A (3 mg at 37 °C for 1 h) and proteinase K (5 mg, 18 h at 37 °C). DNA was isolated by phenol/chloroform extraction and precipitated with ethanol/sodium acetate. DNA amounts were estimated by UV and accurately quantified followed by HPLC analysis of dG in enzymatic digests.[40]

Quantitation of O^6-POB-G Adducts in HBEC DNA treated with NNKOAc

DNA isolated from HBEC cells (32–36 μg) was dissolved in 100 μl water and spiked with D_4-O^6-pob-dG (3 pmol, internal standard for mass spectrometry). O^6-POB-G was quantified by capillary HPLC-ESI^+-MS/MS following acid hydrolysis and SPE purification as described elsewhere.[31]

Statistical Analysis

All statistical analyses were carried out by the University of Minnesota Masonic Cancer Center Biostatistics Core. Time course repair experiments were analyzed using a linear regression model, which included a linear term for time and a factor for methylation condition or O^6-POB-G position, depending on the experiments. All pairwise comparisons were considered and a Bonferroni adjustment was used to control for multiple comparisons. A similar analysis was completed for the association between AGT protein concentration and % unbound DNA (EMSA assays) with the only difference being that a quadratic relationship between AGT protein concentration and % unbound DNA was considered instead of a linear relationship. A one-way analysis of variance (ANOVA) was used to compare the extent of AGT-mediated repair for O^6-POB-G placed at different positions within *K-ras* gene derived DNA sequence. All pairwise comparisons were again considered and the Bonferroni adjustment was used to control for multiple comparisons. Finally, p-values less than 0.05 were considered significant and all analyses were completed in R version 2.15.1. Statistical results are given in the Supporting Information.

Results

Selection of DNA Sequences and Characterization of Synthetic DNA Duplexes

DNA sequences selected for this study (Tables 1 and 2) were derived from codons 8–15 of the *K-ras* protooncogene and two regions of the *p53* tumor suppressor gene containing codons 158, 245 and 248. *K-ras* codon 12 and *p53* codons 158, 245, and 248 are frequently mutated in smoking-induced lung cancer, supposedly a result of preferential tobacco-carcinogen-DNA adduct formation, deficient repair, and selection processes.[43,44] Synthetic DNA oligodeoxynucleotides containing site-specific O^6-POB-G adducts were prepared by

solid phase synthesis from the corresponding nucleoside phosphoramidites[34] and purified by reverse phase HPLC. Each strand was characterized by HPLC-ESI$^-$ MS (Table 1). To generate double stranded DNA, each oligomer was annealed to the complementary strand containing cytosine opposite O^6-POB-dG. Since cytosine residues within CG dinucleotides of the *p53* gene are endogenously methylated in mammalian cells,[24] a range of *p53* codon 158, 245, and 248 sequences were investigated containing cytosine or 5-methylcytosine (^{Me}C) immediately 5′ and/or in the base paired position to O^6-POB-G (Table 2).

The thermodynamic stability of O^6-POB-dG containing DNA duplexes was characterized by UV melting. All structurally modified duplexes produced hyperbolic thermal melting curves consistent with the formation of B-form DNA (see Supporting Information S-1). For *p53* gene derived sequences, the introduction of ^{Me}C increased UV melting temperature by 0.2 – 2°C, indicative of an enhanced duplex stability (Table 2). This is consistent with our previous studies, where 0.9 – 3.2 °C increases in UV melting temperatures were observed upon single C-5 cytosine methylation.[30,45–47] ^{Me}C increases DNA duplex stability due to enhanced π-π stacking interactions of C-5 methylated cytosine with neighboring DNA nucleobases.[48–50] Overall, our UV melting studies confirm that O^6-POB-dG containing DNA strands (Table 1) form standard B-form duplexes, which are stabilized by the presence of ^{Me}C.

HPLC-ESI-MS/MS Approach to Follow the Kinetics of AGT-mediated Repair

The kinetics of AGT-mediated dealkylation of O^6-POB-G as a function of DNA sequence context was investigated using accurate and precise isotope dilution HPLC-ESI$^+$-MS/MS methodology recently developed in our laboratory.[31] In brief, DNA duplexes containing site specific O^6-POB-G were incubated with human recombinant AGT protein under second order reaction conditions (DNA:protein molar ratio = 1.25) for specified periods of time, and the reactions were quenched with hydrochloric acid (Figure 1). We chose to study the kinetics of repair using second order kinetics because of the stoichiometric nature of AGT-mediated dealkylation (see above), which acts as a reactant rather than an enzyme.[14] Following spiking with D_4-O^6-POB-dG (internal standard for mass spectrometry), DNA was subjected to mild acid hydrolysis to release O^6-POB-G, and the amounts of O^6-POB-G remaining in DNA after repair reaction were determined by HPLC-ESI$^+$-MS/MS using D_4-O^6-POB-G internal standard (Figure 2).[31]

Kinetics of AGT-mediated O^6-POB-G Repair as a Function of DNA Sequence Context

To determine whether DNA sequence context affects the efficiency of AGT-mediated repair of O^6-POB-G adducts, *K-ras* derived DNA duplexes were prepared (5′-G_1TA G_2TT G_3G_4A G_5CT G_6G_7T G_8G_9C G_{10}T-3′) where G3, G4, G5, G6, or G7 were replaced with O^6-POB-dG) (Table 1). Duplexes containing site-specific adduct were incubated with human recombinant AGT protein under second order conditions, and the unrepaired adducts were quantified by HPLC-ESI$^+$-MS/MS as described above. The extent of O^6-POB-G repair at time t (E_t) was calculated as shown in equation 3:

$$E_t = \frac{X_0 - X_t}{X_0} * 100\% \quad (3)$$

where X_0 and X_t are the amounts of O^6-POB-G adducts remaining in DNA at time = 0 sec and time = t sec, respectively.

We found that the extent of AGT repair of O^6-POB-dG adducts located at G3, G4, G5, G6 and G7 following 15 s reaction varied between 2.6% and 28.9%, depending on sequence position (Figure 3). AGT repair was most efficient at G5 (28.9%, *K-ras* codon 11, A<u>G</u>C

context), while the lowest amount of AGT-mediated dealkylation occurred at G3 (*K-ras* codon 8, TGG context). O^6-POB-dG adducts present at G4 (codon 9), G6 (codon 12), and G7 (codon 12) exhibited intermediate AGT reactivity (8.4–13.5%) (Figure 3).

Since G6 and G7 are located within a known *K-ras* mutations "hotspot" (codon 12, GGT → GTT, GTT)[51], a more comprehensive kinetic analysis was conducted for these two sites. DNA duplexes 5′-G_1TA G_2TT G_3G_4A G_5CT G_6G_7T G_8G_9C G_{10}T-3′ containing O^6-POB-G at G6 or G7 (N = 5) were allowed to react with AGT for 5 - 60 sec, and O^6-POB-G amounts repaired at time *t* were plotted versus time (Figure 4). The kinetic curves were fitted to the 2nd order quadratic equation (equation (1) above) to obtain the second order rates of repair. Based on these data, the second order reaction rates for AGT repair of O^6-POB-dG adducts present at G_6 and G_7 were calculated as $8.2 \pm 0.3 \times 10^5$ $M^{-1}s^{-1}$ and $1.64 \pm 0.1 \times 10^6$ $M^{-1}s^{-1}$, respectively. These differences in dealkylation rates were statistically significant ($p < 0.001$, Supporting Information S-2). Taken together, our results indicate that DNA sequence context has a considerable effect on the efficiency of AGT-mediated repair of O^6-POB-dG adducts.

Kinetics of AGT-mediated Repair of O^6-POB-G as a Function of Cytosine Methylation

Previous studies have suggested that endogenous cytosine methylation within CG dinucleotides of the *p53* gene may influence the rates of AGT repair of O^6-alkylgunaine adducts present at these sites.[30] To determine whether the rate of O^6-POB-G repair by AGT are affected by methylation status of neighboring cytosine, we conducted second order kinetic analysis of AGT-mediated dealkylation reaction for O^6-POB-G adducts placed within unmethylated, hemimethylated, and fully methylated CG dinucleotides representing *p53* codons 158, 245 and 248 (Table 2). We found that AGT repair efficiency was only weakly affected by cytosine methylation status (Table 3 and Figure 5). For example, for O^6-POB-G adducts located within *p53* codon 248, the observed second order dealkylation rates were $3.09 \pm 0.16 \times 10^6$ M^{-1} s^{-1} (unmethylated CG dinucleotide), $3.82 \pm 0.12 \times 10^6$ M^{-1} s^{-1} (5′-^{Me}C), $2.65 \pm 0.15 \times 10^6$ M^{-1} s^{-1} (base paired ^{Me}C), and $2.94 \pm 0.14 \times 10^6$ M^{-1} s^{-1} (fully methylated CG dinucleotide) (see Figure 5A and Table 3). Similar results were obtained for O^6-POB-G adducts placed within the context of *p53* codon 158 (Table 2 and Figure 5B) and *p53* codon 245 (Table 3 and Figure 5C). Statistical results are given in Supplement S-2.

AGT Protein Binding to O^6-POB-G-Containing DNA duplexes

To investigate AGT protein binding to O^6-POB-G-containing DNA, electrophoretic mobility shift assays were conducted with purified AGT protein and site specifically modified DNA duplexes derived from *p53* codons 248, 158, and 245 and surrounding sequences (Table 4). AGT active site mutant (C145A) was employed in these studies since the presence of C145A mutation preserves the affinity of AGT protein for DNA, but makes the protein variant unable to participate in the alkyl transfer reaction.[52]

Following incubation of radiolabeled O^6-POB-G-containing duplexes with increasing amounts of C145A AGT protein (AGT: DNA ratios 0–7.5), AGT-DNA complexes were detected as a slowly moving band on a non-denaturing polyacrylamide gel (Figure 6). AGT-DNA dissociation constants (K_d) were obtained from the plots of $[D]/[D]_T$ vs. $[P]_T$ where [D], $[D]_T$ and $[P]_T$ are molar concentrations of O^6-POB-G containing DNA, bound and unbound DNA, and AGT protein, respectively.[30] Calf thymus DNA was added to the incubation mixtures to minimize any non-specific binding interactions between the protein and O^6-POB-G containing DNA duplexes.[42]

Dissociation constant (K_d) values calculated for AGT-DNA complexes containing O^6-POB-G (Table 4, Supplement S4) were similar to AGT-DNA dissociation constants previously reported for O^6-Me-G containing DNA,[30] suggesting that O^6-alkyl group identity does not influence the dynamics of AGT-DNA interactions. The affinity of AGT protein for DNA duplexes containing O^6-POB-G in *p53* codon 248 sequence context was moderately affected by the presence of ^{Me}C, with K_d values of $2.2 \pm 0.2 \times 10^{-6}$ M, $2.0 \pm 0.2 \times 10^{-6}$ M, $1.8 \pm 0.3 \times 10^{-6}$ M, and $1.0 \pm 0.1 \times 10^{-6}$ M observed for unmethylated DNA, ^{Me}C[O^6-POB-G]sequence, O^6-POB-G: ^{Me}C base pair, and fully methylated C[O^6-POB-G] dinucleotides ($p < 0.001$), respectively (Table 4). The presence of 5′-^{Me}C decreased AGT binding affinity towards O^6-POB-G adducts within *p53* codon 158 ($K_d = 4.8 \pm 0.5 \times 10^{-6}$ M) as compared to the corresponding unmethylated DNA duplex ($K_d = 2.3 \pm 0.2 \times 10^{-6}$ M, $p < 0.001$). In contrast, cytosine methylation did not affect AGT binding to the DNA duplex derived from *p53* codon 245 ($K_d = 1.3 \pm 0.3 \times 10^{-6}$ M – $1.5 \pm 0.1 \times 10^{-6}$ M, Table 4 and Supplementary Table S4).

O^6-POB-G Adduct Formation and Repair in Human Bronchial Epithelial Cells (HBEC)

As described above, NNK and NNN are widely recognized as causative agents of human lung cancer.[53] Following metabolic activation to methylating and pyridyloxobutylating agents (Scheme 1), tobacco specific nitrosamines present in tobacco smoke damage DNA within epithelial cells of the pulmonary airways, ultimately leading to mutations in critical genes and lung cancer initiation.[54] DNA repair systems can prevent malignant transformation by removing NNK-induced DNA lesions from DNA before they can be converted to heritable mutations (Scheme 2). Urban et al. conducted a comprehensive study of the formation and repair of pyridyloxobutylated DNA adducts in tissues of laboratory mice treated with a pyridyloxo-butylating agent (NNKOAc).[11] These authors reported that O^6-POB-G adducts persisted in mouse lung at significant levels for up to 96 h post-treatment, and that AGT depletion with O^6-benzylguanine led to a 2-fold increase in O^6-POB-G adduct levels.[11] However, to our knowledge, the ability of human bronchial epithelial cells to repair O^6-POB-G lesions and the respective role of AGT in their repair remains had not been elucidated. This is important given the documented species differences in POB-DNA adducts formation and repair.[11]

To study the kinetics of O^6-POB-dG repair in human lung cells, normal immortalized human bronchial epithelial cells (HBEC) in culture were treated with model pyridyloxo-butylating agent, 4-acetoxynethylnitrosamino)-1-(3-pyridyl)-1-butanone (NNKOAc). Esterase catalyzed hydrolysis of NNKOAc generates the same intermediate, pyridyloxobutyl diazohydroxide, that also forms upon metabolic activation of NNK and forms O^6-POB-dG adducts in DNA (Scheme 1).[1] Preliminary studies have shown that HBEC cell treatment with 150 μM NNKOAc for 1 h minimally affected cell viability (Supplement S-5). Following carcinogen removal, cells were allowed to recover over 1–12 h. DNA was extracted, and the amounts of O^6-POB-dG adducts remaining in DNA at each time point were determined by isotope dilution HPLC ESI$^+$-MS/MS (Figure 2). The same experiment was conducted in the presence of AGT inhibitor (O^6-benzylguanine) to evaluate potential contribution of AGT repair pathway to adduct removal in human bronchial epithelial cells.

We found that DNA of HBEC cells treated with 150 μM NNKOAc for 1 h contained 14.5 O^6-POB-dG adducts/10^7 nucleotides (Figure 7). The number of adducts was significantly greater in cells treated in the presence of AGT-inhibitor, O^6-benzylguanine (20.7 adducts/10^7 nucleotides). In the absence of O^6-bz-G, O^6-POB-dG adducts were gradually repaired, with approximately 5 adducts/10^7 nucleotides remaining after 12 h of repair incubation (Figure 7). In contrast, adduct numbers remained essentially unchanged in cells treated with AGT inhibitor O^6-benzylguanine (Figure 7), suggesting that AGT plays an important role in protecting human bronchial cells against pyridyloxobutylation damage.

Discussion

O^6-POB-dG adducts induced by tobacco-specific nitrosamines NNK and NNN appear to play an important role in the etiology of smoking-induced lung cancer.[55,56] A/J mice treated with model pyridyloxobutylating compound, 4-acetoxynethylnitrosamino)-1-(3-pyridyl)-1-butanone (NNKOAc), develop lung tumors.[8,11] Furthermore, pyridyloxobutylated DNA adducts accumulate in pulmonary type II cells of rats treated with NNK and in pulmonary tissues of lung cancer patients.[57,58] Site-specific mutagenesis experiments have revealed the ability of O^6-POB to induce G to T and G to A mutations,[6,9] and the same types of mutations predominate in smoking induced lung tumors.[32,44] G to T and G to A base substitutions in the *K-ras* protooncogene are observed in lung tumors of mice treated with NNKOAc.[8] Furthermore, O^6-POB has been shown to inhibit AGT repair of other NNK-induced DNA adducts such as O^6-methyl-dG.[59]

Direct removal of the O^6-POB group by O^6-alkylguanine DNA alkyltransferase (AGT) appears to be the main repair pathway for O^6-POB-dG adducts in cells. AGT appears to protect cells from mutagenic effects of O^6-POB-dG.[6] Studies in Chinese hamster ovary (CHO) cell lines deficient in specific repair pathways have shown that O^6-POB-dG adducts were efficiently repaired in CHO cells expressing AGT, but persisted in AGT deficient cells.[60] In animal studies, co-administration of NNKOAc and AGT inhibitor O^6-benzylguanine significantly increased O^6-POB-dG adduct concentrations in tissues, although additional repair pathways appear to exist.[11] Unlike other bulky O^6-alkylguanine adducts, O^6-POB-dG was a poor substrate for human nucleotide excision repair pathway (NER).[60]

The rates of AGT-mediated repair of O^6-POB-dG lesions can be affected by the local DNA sequence context, [21,23,61–63] leading to adduct accumulation at specific sites within the genome. For example, Coulter et. al. reported that the first order rate for AGT-mediated repair of O^6-POB-dG placed in the first position of the *H-ras* codon 12 (5′- [O^6-POB-dG]GA-3′, 0.95×10^{-4} s^{-1}) was ~ 6 times higher than when the adduct was placed at the second position of codon 12 (5′ G[O^6-POB-dG]A -3′, 0.16×10^{-4} s^{-1}).[21] Similar results were obtained by Mijal et. al.,[22] who measured the relative rates of AGT-mediated repair of O^6-POB-dG adducts as compared to O^6-Me-dG in *H-ras* derived sequence using a gel electrophoresis-based approach. O^6-POB-dG was repaired faster when it was placed opposite thymine rather than paired with cytosine.[22] However, to our knowledge, the kinetics of O^6-POB-dG repair in other sequence contexts has not been previously investigated.

In the present work, a systematic study of sequence-dependent repair of O^6-POB-dG by AGT was undertaken. DNA duplexes representing codons 8–13 of *K-ras* protooncogene were selected (Table 1). *K-ras* is frequently mutated in lung tumors of smokers, specifically exhibiting G → A transitions and G → T transversions within codon 12.[64–67] The same genetic changes are observed in lung tumors of laboratory animals treated with tobacco smoke carcinogen, NNK.[8] We employed a mass spectrometry based assay developed in our laboratory[31] to enable accurate and specific quantification of O^6-POB-dG remaining in DNA as a function of repair time (Figures 1,2). We found that the efficiency of AGT mediated O^6-POB group transfer was affected by local sequence context, with ~ 10-fold faster repair observed at G5 (A<u>G</u>C) than at the G3 (T*G*G) (Figure 3) Second order repair rates for O^6-POB-dG placed within the first and 2nd positions of *K-ras* codon 12 were 8.2 and 16.4×10^5 $M^{-1}s^{-1}$, respectively (Figure 4). By comparison, the rates of repair of O^6-Me-dG adducts present at the same positions were 1.4×10^7 $M^{-1}s^{-1}$ and 7.4×10^6 $M^{-1}s^{-1}$, respectively.[37] These results indicate that O^6-POB-dG repair by AGT is much slower than that of O^6-Me-dG and shows a greater dependence on local sequence environment. This can

be explained by steric effects of the bulky pyridyloxobutyl group, which may interfere with correct placement of the adduct within the protein active site, inhibiting alkyl transfer.[14]

In contrast, AGT repair of O^6-POB-dG adducts was relatively unaffected by neighboring 5-methylcytosine (^{Me}C). ^{Me}C is an important endogenous DNA modification that plays an major role in many cellular processes.[68] All CG dinucleotides within the coding sequence of the *p53* tumor suppressor gene are methylated, and the same sites are frequently mutated in smoking-induced lung cancer.[24,69] Methylation of the C-5 position of cytosine can influence the local DNA structure and the electronic environment within ^{Me}CG dinucleotides.[70]

To investigate the potential effects of cytosine methylation on O^6-POB-G repair,site-specific adducts were placed within unmethylated, hemimethylated, and fully methylated CG dinucleotides within *p53* codons 158, 245 and 248 (Table 3). Following incubation with AGT protein, the second order rates for AGT mediated alkyl transfer were determined by HPLC-ESI$^+$-MS/MS. We found that the kinetics of AGT-mediated O^6-POB-dG repair was only weakly affected by neighboring ^{Me}C (Figure 5, Table 3). Gel shift experiments revealed that AGT binding to pyridyloxobutylated DNA was not influenced by cytosine methylation (Table 4). This is not unexpected since the 5-methyl group on cytosine is projected into DNA major groove,[46] while AGT binds to the minor groove of DNA.[12] Other authors previously noted that that AGT binding to O^6-alkylguanine containing DNA duplexes was not dependent on DNA sequence context or the alkyl group identity, but was increased in the presence of O^6-alkylguanine adducts as compared to unmodified DNA.[30,63,71]

We investigated the kinetics of O^6-POB-dG adduct repair in normal human bronchial epithelial cells (HBEC) since these cells are targeted by nitrosamines present in tobacco smoke. Previous studies have shown that human bronchial epithelial cells in culture can be malignantly transformed following treatment with NNK (100 or 400 mg/ml) for 7 days.[72] Our results provide evidence for the ability of HBEC cells to repair O^6-POB-dG (Figure 7). Since the rate of repair was significantly reduced in the presence of AGT inhibitor (O^6-benzylguanine), we conclude that AGT repair may play an important role in preventing tobacco nitrosamine-associated lung cancer.

In conclusion, our results indicate that while local DNA sequence context influences the efficiency of O^6-POB-G repair in the context of *K-ras* protooncogene, the presence of ^{Me}C does not influence AGT protein binding to and repair of pyridyloxobutylated DNA. Since our experiments with human bronchial epithelial cells (Figure 7) indicate that direct repair by AGT plays an important role in the removal of O^6-POB-G adducts from human bronchial epithelial cells, sequence dependent AGT repair may lead to accumulation of pyridyloxobutylating adducts and increased mutagenesis at inefficiently repaired sites.

Supplementary Material

Refer to Web version on PubMed Central for supplementary material.

Acknowledgments

Funding Support

This work was funded by grants from the National Cancer Institute (CA-095039 (N.T.) and CA-018137 (S.K.)) and a Grant-in-Aid Grant from the University of Minnesota Graduate School (F.K.).

We thank Professor Stephen S. Hecht (University of Minnesota Cancer Center) for his generous gift of D_4-O^6-POB-dG internal standard and Brock Matter (Analytical Biochemistry and Mass Spectrometry Facility at the Cancer Center, University of Minnesota) for his assistance with mass spectrometry experiments. We are grateful to

Robert Carlson (University of Minnesota Masonic Cancer Center) for preparing the tables and figures for this manuscript.

Abbreviations

AGT	O^6-alkylguanine-DNA-alkyltransferase
BSA	bovine serum albumin
O^6-Bz-dG	O^6-benzyl-deoxyguanosine
O^6-Bz-G	O^6-Benzylguanine
DTT	dithiothreitol
DNase I	deoxyribonuclease I
EDTA	ethylenediamine tetraacetic acid
HPLC-ESI-MS/MS	high performance liquid chromatography-electrospray ionization-tandem mass spectrometry
HBEC	human bronchial epithelial cells
N7-MeG	N7-methylguanine
O^6-Me-dG	O^6-methyl-2′-deoxyguanosine
O^6-Me-G	O^6-methylguanine
PAGE	polyacrylamide gel electrophoresis
N7-POB-G	N7-[4-oxo-4-(3-pyridyl)-but-1-yl]guanine
NNK	4-(methylnitrosamino)-1-(3-pyridyl)-1-butanone
NNN	N-nitrosonicotine
O^6-POB-dG	O^6-[4-oxo-4-(3-pyridyl)but-1-yl]deoxyguanosine
D_4-O^6-POB-dG	D_4-O^6-[4-oxo-4-(3-pyridyl)but-1-yl]deoxyguanosine
O^6-POB-G	O^6-[4-oxo-4-(3-pyridyl)but-1-yl]guanine
PDE I	phosphodiesterase I
PDE II	phosphodiesterase II
POB	pyridyloxobutyl
SPE	solid phase extraction
TEAOAc	triethylamonium acetate
PNK	polynucleotide kinase

Reference List

1. Hecht SS. DNA adduct formation from tobacco-specific N-nitrosamines. Mutat Res. 1999; 424:127–142. [PubMed: 10064856]
2. Hecht SS. Biochemistry, biology, and carcinogenicity of tobacco-specific N- nitrosamines. Chem Res Toxicol. 1998; 11:559–603. [PubMed: 9625726]
3. Hecht SS, Trushin N, Castonguay A, Rivenson A. Comparative tumorigenicity and DNA methylation in F344 rats by 4-(methylnitrosamino)-1-(3-pyridyl)-1-butanone and N-nitrosodimethylamine. Cancer Res. 1986; 46:498–502. [PubMed: 3940627]

4. Hecht SS, Spratt TE, Trushin N. Evidence for 4-(3-pyridyl)-4-oxobutylation of DNA in F344 rats treated with the tobacco-specific nitrosamines 4-(methylnitrosamino)-1-(3- pyridyl)-1-butanone and N′-nitrosonornicotine. Carcinogenesis. 1988; 9:161–165. [PubMed: 3335041]
5. Peterson LA, Hecht SS. O^6-Methylguanine is a critical determinant of 4-(methylnitrosamino)-1-(3-pyridyl)-1-butanone tumorigenesis in A/J mouse lung. Cancer Res. 1991; 51:5557–5564. [PubMed: 1913675]
6. Mijal RS, Loktionova NA, Vu CC, Pegg AE, Peterson LA. O^6-pyridyloxobutylguanine adducts contribute to the mutagenic properties of pyridyloxobutylating agents. Chem Res Toxicol. 2005; 18:1619–1625. [PubMed: 16533027]
7. Upadhyaha P, Lindgren BR, Hecht SS. Comparative levels of O^6-methylguanine, pyridyloxobutyl-, and pyridylhydroxybutyl-DNA adducts in lung and liver of rats treated chronically with tobacco-specific carcinogen 4-(methylnitrosamino)-1-(3-pyridyl)-1-butanone. Drug Metab Dispos. 2009; 37:1147–1151. [PubMed: 19324941]
8. Ronai ZA, Gradia S, Peterson LA, Hecht SS. G to A transitions and G to T transversions in codon 12 of the *Ki-ras* oncogene isolated from mouse lung tumors induced by 4- (methylnitrosamino)-1-(3-pyridyl)-1-butanone (NNK) and related DNA methylating and pyridyloxobutylating agents. Carcinogenesis. 1993; 14:2419–2422. [PubMed: 7902220]
9. Pauly GT, Peterson LA, Moschel RC. Mutagenesis by O^6-[4-oxo-4-(3-pyridyl)butyl]guanine in *Escherichia coli* and human cells. Chem Res Toxicol. 2002; 15:165–169. [PubMed: 11849042]
10. Loechler EL, Green CL, Essigmann JM. *In vivo* mutagenesis by O^6-methylguanine built into a unique site in a viral genome. Proc Natl Acad Sci U S A. 1984; 81:6271–6275. [PubMed: 6093094]
11. Urban AM, Upadhyaya P, Cao Q, Peterson LA. Formation and repair of pyridyloxobutyl DNA adducts and their relationship to tumor yield in A/J mice. Chem Res Toxicol. 2012; 25:2167–2178. [PubMed: 22928598]
12. Daniels DS, Woo TT, Luu KX, Noll DM, Clarke ND, Pegg AE, Tainer JA. DNA binding and nucleotide flipping by the human DNA repair protein AGT. Nat Struct Mol Biol. 2004; 11:714–720. [PubMed: 15221026]
13. Pegg AE. Repair of O^6-alkylguanine by alkyltransferases. Mutat Res. 2000; 462:83–100. [PubMed: 10767620]
14. Pegg AE. Multifaceted roles of alkyltransferase and related proteins in DNA repair, DNA damage, resistance to chemotherapy, and research tools. Chem Res Toxicol. 2011; 24:618–639. [PubMed: 21466232]
15. Daniels DS, Mol CD, Arvai AS, Kanugula S, Pegg AE, Tainer JA. Active and alkylated human AGT structures: a novel zinc site, inhibitor and extrahelical base binding. EMBO J. 2000; 19:1719–1730. [PubMed: 10747039]
16. Tubbs JL, Pegg AE, Tainer JA. DNA binding, nucleotide flipping, and the helix-turn-helix motif in base repair by O^6-alkylguanine-DNA alkyltransferase and its implications for cancer chemotherapy. DNA Repair. 2007; 6:1100–1115. [PubMed: 17485252]
17. Fried MG, Kanugula S, Bromberg JL, Pegg AE. DNA Binding Mechanism of O^6-alkylguanine-DNA-alkyltransferase: Stoichiometry and effects of DNA base composition and secondary structure on complex stability. Biochemistry. 1996; 35:15295–15301. [PubMed: 8952480]
18. Major GN, Brady M, Notarianni GB, Collier JD, Douglas MS. Evidence for ubiquitin-mediated degradation of the DNA repair enzyme for O^6-methylguanine in non-tumor derived human cell and tissue extracts. Biochem Soc Trans. 1997; 25:359S. [PubMed: 9191404]
19. Tessmer I, Melikishvili M, Fried MG. Cooperative cluster formation, DNA bending and base-flipping by O6-alkylguanine-DNA alkyltransferase. Nucleic Acids Res. 2012; 40:8296–8308. [PubMed: 22730295]
20. Rasimas JJ, Kar SR, Pegg AE, Fried MG. Interactions of human O^6-alkylguanine-DNA alkyltransferase (AGT) with short single-stranded DNAs. Journal of Biological Chemistry. 2007; 282:3357–3366. [PubMed: 17138560]
21. Coulter R, Blandino M, Tomlinson JM, Pauly GT, Krajewska M, Moschel RC, Peterson LA, Pegg AE, Spratt TE. Differences in the rate of repair of O^6-alkylguanines in different sequence contexts

by O^6-alkylguanine-DNA alkyltransferase. Chem Res Toxicol. 2007; 20:1966–1971. [PubMed: 17975884]

22. Mijal RS, Kanugula S, Vu CC, Fang Q, Pegg AE, Peterson LA. DNA sequence context affects repair of the tobacco-specific adduct O^6-[4-oxo-4-(3-pyridyl)butyl]guanine by human O^6-alkylguanine-DNA alkyltransferase. Cancer Res. 2006; 66:4968–4974. [PubMed: 16651455]
23. Meyer AS, McCain MD, Fang Q, Pegg AE, Spratt TE. O^6-alkylguanine-DNA alkyltransferases repair *O6*-methylguanine in DNA with Michaelis-Menten-like kinetics. Chem Res Toxicol. 2003; 16:1405–1409. [PubMed: 14615965]
24. Tornaletti S, Pfeifer GP. Complete and tissue-independent methylation of CpG sites in the *p53* gene: implications for mutations in human cancers. Oncogene. 1995; 10:1493–1499. [PubMed: 7731703]
25. Hussain SP, Hollstein MH, Harris CC. *p53* tumor suppressor gene: at the crossroads of molecular carcinogenesis, molecular epidemiology, and human risk assessment. Ann N Y Acad Sci. 2000; 919:79–85. [PubMed: 11083100]
26. Greenblatt MS, Bennett WP, Hollstein M, Harris CC. Mutations in the *p53* tumor suppressor gene: clues to cancer etiology and molecular pathogenesis. Cancer Res. 1994; 54:4855–4878. [PubMed: 8069852]
27. Hollstein M, Shomer B, Greenblatt M, Soussi T, Hovig E, Montesano R, Harris CC. Somatic point mutations in the *p53* gene of human tumors and cell lines: updated compilation. Nucleic Acids Res. 1996; 24:141–146. [PubMed: 8594564]
28. Hernandez-Boussard T, Rodriguez-Tome P, Montesano R, Hainaut P. IARC *p53* mutation database: a relational database to compile and analyze *p53* mutations in human tumors and cell lines. International Agency for Research on Cancer. Hum Mutat. 1999; 14:1–8. [PubMed: 10447253]
29. Wolf P, Hu YC, Doffek K, Sidransky D, Ahrendt SA. O^6-methylguanine-DNA methyltransferase promoter hypermethylation shifts the *p53* mutational spectrum in non small cell lung cancer. Cancer Res. 2001; 61:8113–8117. [PubMed: 11719438]
30. Guza R, Ma L, Fang Q, Pegg AE, Tretyakova NY. Cytosine methylation effects on the repair of O^6-methylguanines within CG dinucleotides. J Biol Chem. 2009; 284:22601–22610. [PubMed: 19531487]
31. Kotandeniya D, Murphy D, Seneviratne U, Guza R, Pegg A, Kanugula S, Tretyakova N. Mass spectrometry based approach to study the kinetics of O^6-alkylguanine DNA alkyltransferase-mediated repair of O^6-pyridyloxobutyl-2′-deoxyguanosine adducts in DNA. Chem Res Toxicol. 2011; 24:1966–1975. [PubMed: 21913712]
32. Pfeifer GP. *p53* mutational spectra and the role of methylated CpG sequences. Mutat Res. 2000; 450:155–166. [PubMed: 10838140]
33. Wang L, Spratt TE, Liu XK, Hecht SS, Pegg AE, Peterson LA. Pyridyloxobutyl adduct O^6-[4-oxo-4-(3-pyridyl)butyl]guanine is present in 4-(acetoxymethylnitrosamino)-1-(3-pyridyl)-1-butanone-treated DNA is a substrate for O^6-alkylguanine-DNA alkyltransferase. Chem Res Toxicol. 1997; 10:562–567. [PubMed: 9168254]
34. Wang L, Spratt TE, Pegg AE, Peterson LA. Synthesis of DNA oligonucleotides containing site-specifically incorporated O^6-[4-oxo-4-(3-pyridyl)butyl]guanine and their reaction with O^6-alkylguanine-DNA alkyltransferase. Chem Res Toxicol. 1999; 12:127–131. [PubMed: 10027788]
35. Liu L, Xu-Welliver M, Kanugula S, Pegg AE. Inactivation and degradation of O^6-alkylguanine-DNA alkyltransferase after reaction with nitric oxide. Cancer Res. 2002; 62:3037–3043. [PubMed: 12036910]
36. Edara S, Kanugula S, Goodtzova K, Pegg AE. Resistance of the human O^6-alkylguanine-DNA alkyltransferase containing arginine at codon 160 to inactivation by O^6-benzylguanine. Cancer Res. 1996; 56:5571–5575. [PubMed: 8971155]
37. Guza R, Rajesh M, Fang Q, Pegg AE, Tretyakova N. Kinetics of O^6-Me-dG repair by O^6-alkylguanine DNA-alkyltransferase within *K-ras* gene derived DNA sequences. Chem Res Toxicol. 2006; 19:531–538. [PubMed: 16608164]
38. Ziegel R, Shallop A, Upadhyaya P, Jones R, Tretyakova N. Endogenous 5-methylcytosine protects neighboring guanines from N7 and O^6-methylation and O^6-pyridyloxobutylation by the tobacco

carcinogen 4-(methylnitrosamino)-1-(3-pyridyl)-1-butanone. Biochemistry. 2004; 43:540–549. [PubMed: 14717610]

39. Rajesh M, Wang G, Jones R, Tretyakova N. Stable isotope labeling-mass spectrometry analysis of methyl- and pyridyloxobutyl-guanine adducts of 4-(methylnitrosamino)-1-(3-pyridyl)-1-butanone in *p53*-derived DNA sequences. Biochemistry. 2005; 44:2197–2207. [PubMed: 15697245]
40. Matter B, Wang G, Jones R, Tretyakova N. Formation of diastereomeric benzo[*a*]pyrene diol epoxide-guanine adducts in *p53* gene-derived DNA sequences. Chem Res Toxicol. 2004; 17:731–741. [PubMed: 15206894]
41. Rasimas JJ, Pegg AE, Fried MG. DNA-binding mechanism of O^6-alkylguanine-DNA alkyltransferase. Effects of protein and DNA alkylation on complex stability. J Biol Chem. 2003; 278:7973–7980. [PubMed: 12496275]
42. Spratt TE, Wu JD, Levy DE, Kanugula S, Pegg AE. Reaction and binding of oligodeoxynucleotides containing analogues of O^6-methylguanine with wild-type and mutant human O^6-alkylguanine-DNA alkyltransferase. Biochemistry. 1999; 38:6801–6806. [PubMed: 10346901]
43. Pfeifer GP, Tang M, Denissenko MF. Mutation hotspots and DNA methylation. Curr Top Microbiol Immunol. 2000; 249:1–19. [PubMed: 10802935]
44. Siegfried JM, Gillespie AT, Mera R, Casey TJ, Keohavong P, Testa JR, Hunt JD. Prognostic value of specific KRAS mutations in lung adenocarcinomas. Cancer Epidemiol Biomarkers Prev. 1997; 6:841–847. [PubMed: 9332768]
45. Hausheer FH, Rao SN, Gamcsik MP, Kollman PA, Colvin OM, Saxe JD, Nelkin BD, McLennan IJ, Barnett G, Baylin SB. Computational analysis of structural and energetic consequences of DNA methylation. Carcinogenesis. 1989; 10:1131–1137. [PubMed: 2720906]
46. Zacharias W. Methylation of cytosine influences the DNA structure. Experientia Supplementum. 1993; 64:27–38.
47. Rauch C, Trieb M, Wellenzohn B, Loferer M, Voegele A, Wibowo FR, Liedl KR. C5-methylation of cytosine in B-DNA thermodynamically and kinetically stabilizes BI. J Am Chem Soc. 2003; 125:14990–14991. [PubMed: 14653725]
48. Geacintov NE, Cosman M, Hingerty BE, Amin S, Broyde S, Patel DJ. NMR solution structures of stereoisometric covalent polycyclic aromatic carcinogen-DNA adduct: principles, patterns, and diversity. Chem Res Toxicol. 1997; 10:111–146. [PubMed: 9049424]
49. Norberg J, Vihinen M. Molecular dynamics simulation of the effects of cytosine methylation on structure of oligonucleotides. Journal of Molecular Structure-Theochem. 2001; 546:51–62.
50. Sowers LC, Shaw BR, Sedwick WD. Base stacking and molecular polarizability: effect of a methyl group in the 5-position of pyrimidines. Biochem Biophys Res Commun. 1987; 148:790–794. [PubMed: 3689373]
51. Barbacid M. ras oncogenes: their role in neoplasia. Eur J Clin Invest. 1990; 20:225–235. [PubMed: 2114981]
52. Hazra TK, Roy R, Biswas T, Grabowski DT, Pegg AE, Mitra S. Specific recognition of O^6-methylguanine in DNA by active site mutants of human O^6-methylguanine-DNA methyltransferase. Biochemistry. 1997; 36:5769–5776. [PubMed: 9153417]
53. Hecht SS. Tobacco carcinogens, their biomarkers and tobacco-induced cancer. Nat Rev Cancer. 2003; 3:733–744. [PubMed: 14570033]
54. Hecht SS, Hoffmann D. The relevance of tobacco-specific nitrosamines to human cancer. Cancer Surv. 1989; 8:273–294. [PubMed: 2696581]
55. Peterson LA, Mathew R, Murphy SE, Trushin N, Hecht SS. In vivo and in vitro persistence of pyridyloxobutyl DNA adducts from 4- (methylnitrosamino)-1-(3-pyridyl)-1-butanone. Carcinogenesis. 1991; 12:2069–2072. [PubMed: 1934291]
56. Hecht SS, Isaacs S, Trushin N. Lung tumor induction in A/J mice by the tobacco smoke carcinogens 4- (methylnitrosamino)-1-(3-pyridyl)-1-butanone and benzo[a]pyrene: a potentially useful model for evaluation of chemopreventive agents. Carcinogenesis. 1994; 15:2721–2725. [PubMed: 8001227]
57. Staretz ME, Foiles PG, Miglietta LM, Hecht SS. Evidence for an important role of DNA pyridyloxobutylation in rat lung carcinogenesis by 4-(methylnitrosamino)-1-(3-pyridyl)-1-

butanone: effects of dose and phenethyl isothiocyanate. Cancer Res. 1997; 57:259–266. [PubMed: 9000565]

58. Holzle D, Schlobe D, Tricker AR, Richter E. Mass spectrometric analysis of 4-hydroxy-1-(3-pyridyl)-1-butanone-releasing DNA adducts in human lung. Toxicoclgy. 2007; 232:277–285.
59. Peterson LA, Thomson NM, Crankshaw DL, Donaldson EE, Kenney PJ. Interactions between methylating and pyridyloxobutylating agents in A/J mouse lungs: implications for 4-(methylnitrosamino)-1-(3-pyridyl)-1- butanone-induced lung tumorigenesis. Cancer Res. 2001; 61:5757–5763. [PubMed: 11479212]
60. Li L, Perdigao J, Pegg AE, Lao YB, Hecht SS, Lindgren BR, Reardon JT, Sancar A, Wattenberg EV, Peterson LA. The influence of repair pathways on the cytotoxicity and mutagenicity induced by the pyridyloxobutylation pathway of tobacco-specific nitrosamines. Chemical Research in Toxicology. 2009; 22:1464–1472. [PubMed: 19601657]
61. Dolan ME, Oplinger M, Pegg AE. Sequence specificity of guanine alkylation and repair. Carcinogenesis. 1988; 9:2139–2143. [PubMed: 3180351]
62. Georgiadis P, Smith CA, Swann PF. Nitrosamine-induced cancer: selective repair and conformational differences between O^6-methylguanine residues in different positions in and around codon 12 of rat H-ras. Cancer Res. 1991; 51:5843–5850. [PubMed: 1933853]
63. Bender K, Federwisch M, Loggen U, Nehls P, Rajewsky MF. Binding and repair of O^6-ethylguanine in double-stranded oligonucleotides by recombinant human O^6-alkylguanine-DNA alkyltransferase do not exhibit significant dependance on sequence context. Nucleic Acids Res. 1996; 24:2087–2094. [PubMed: 8668540]
64. Westra WH, Slebos RJ, Offerhaus GJ, Goodman SN, Evers SG, Kensler TW, Askin FB, Rodenhuis S, Hruban RH. *K-ras* oncogene activation in lung adenocarcinomas from former smokers. Evidence that *K-ras* mutations are an early and irreversible event in the development of adenocarcinoma of the lung. Cancer. 1993; 72:432–438. [PubMed: 8319174]
65. Slebos RJ, Rodenhuis S. The ras gene family in human non-small-cell lung cancer. J Natl Cancer Inst Monogr. 1992:23–29. [PubMed: 1327034]
66. Rodenhuis S, Slebos RJ. Clinical significance of *ras* oncogene activation in human lung cancer. Cancer Res. 1992; 52:2665s–2669s. [PubMed: 1562997]
67. Rodenhuis S, Slebos RJ, Boot AJ, Evers SG, Mooi WJ, Wagenaar SS, van Bodegom PC, Bos JL. Incidence and possible clinical significance of *K-ras* oncogene activation in adenocarcinoma of the human lung. Cancer Res. 1988; 48:5738–5741. [PubMed: 3048648]
68. Riggs AD, Jones PA. 5-methylcytosine, gene regulation, and cancer. Adv Cancer Res. 1983; 40:1–30. [PubMed: 6197868]
69. Denissenko MF, Chen JX, Tang MS, Pfeifer GP. Cytosine methylation determines hot spots of DNA damage in the human *p53* gene. Proc Natl Acad Sci U S A. 1997; 94:3893–3898. [PubMed: 9108075]
70. Guza R, Kotandeniya D, Murphy K, Dissanayake T, Lin C, Giambasu GM, Lad RR, Wojciechowski F, Amin S, Sturla SJ, Hudson RH, York DM, Jankowiak R, Jones R, Tretyakova NY. Influence of C-5 substituted cytosine and related nucleoside analogs on the formation of benzo[*a*]pyrene diol epoxide-dG adducts at CG base pairs of DNA. Nucleic Acids Res. 2011; 39:3988–4006. [PubMed: 21245046]
71. Zang H, Fang Q, Pegg AE, Guengerich FP. Kinetic analysis of steps in the repair of damaged DNA by human O^6-alkylguanine-DNA alkyltransferase. J Biol Chem. 2005; 280:30873–30881. [PubMed: 16000301]
72. Zhou H, Calaf GM, Hei TK. Malignant transformation of human bronchial epithelial cells with the tobacco-specific nitrosamine, 4-(methylnitrosamino)-1-(3-pyridyl)-1-butanone. Int J Cancer. 2003; 106:821–826. [PubMed: 12918058]

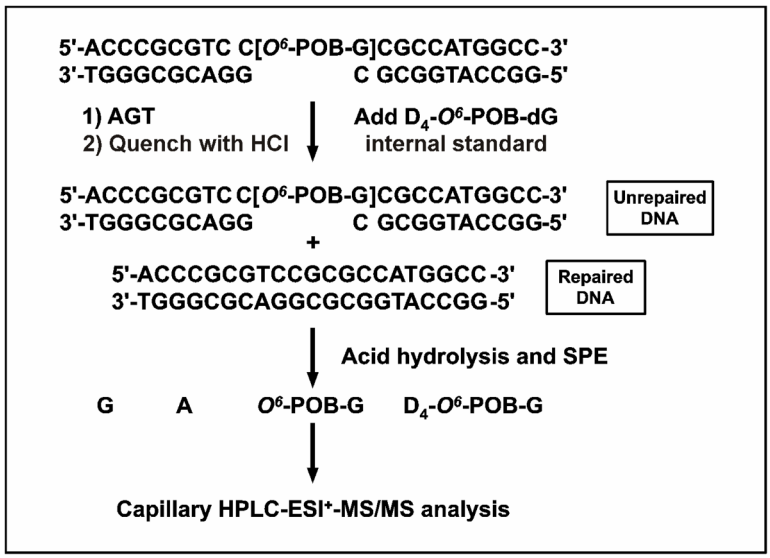

Figure 1.

HPLC-ESI$^+$-MS/MS methodology employed to follow the kinetics of AGT-mediated repair of O^6-POB-G adduct. Following incubation with recombinant AGT protein for specified periods of time, DNA was spiked with d_4-O^6-POB-dG internal standard, subjected to acid hydrolysis to release free base adducts, and analyzed by capillary HPLC-ESI$^+$-MS/MS.

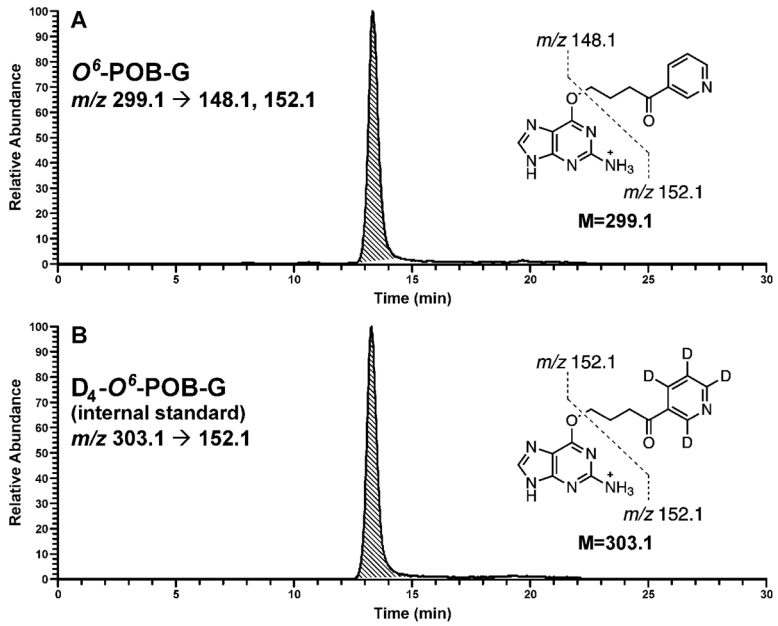

Figure 2.

Representative traces for HPLC-ESI$^+$-MS/MS analyses of O^6-POB-G adducts in DNA hydrolysates. O^6-POB-G and d_4-O^6-POB-G (internal standard) were detected in the SRM mode by monitoring the transitions *m/z* 299.09 [M + H^+] → 148.1 [POB^+], 152.07 [Gua + H^+] for O^6-POB-G (A) and *m/z* 303.09 [M + H^+] → 152.07[D_4-POB^+], [Gua + H^+] for D_4-O^6-POB-G (B).

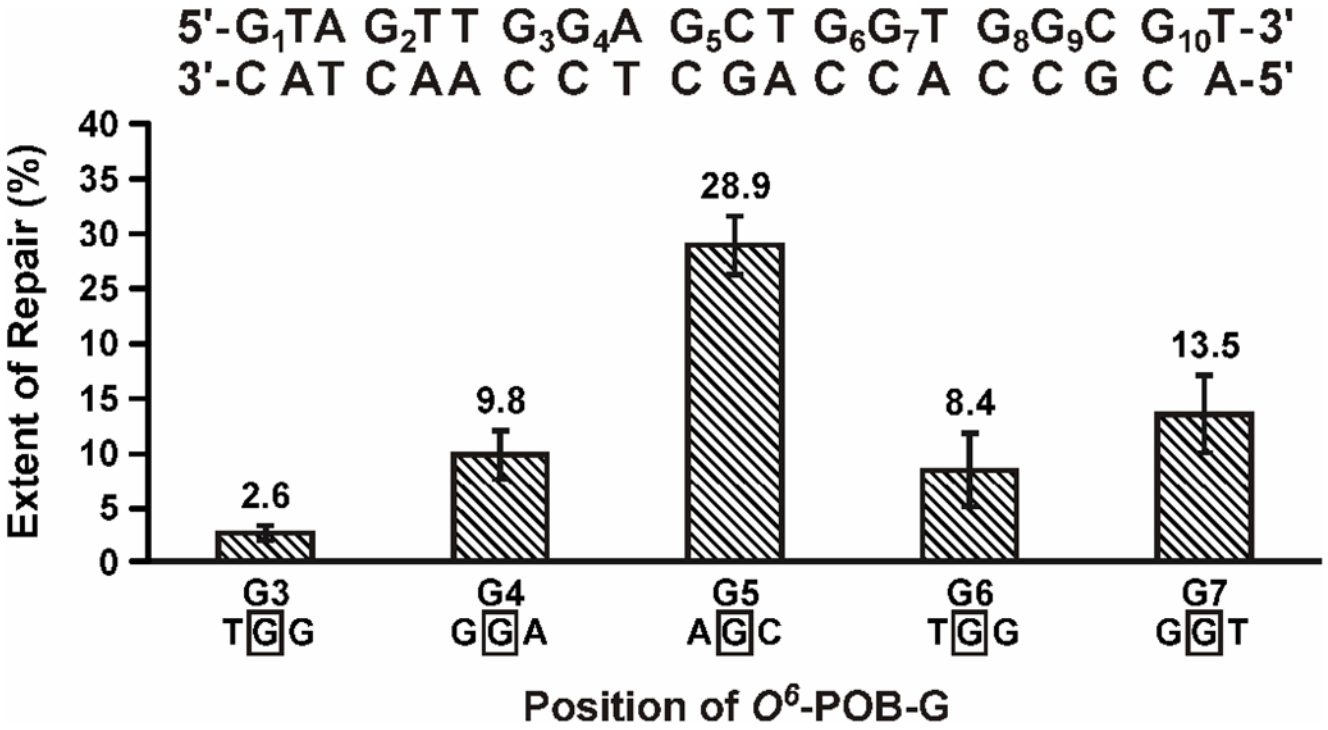

Figure 3.

AGT repair of O^6-POB-dG adducts located at different positions within *K-ras* gene sequence. Synthetic DNA duplexes 5′-G_1TA G_2TT G_3G_4A G_5CT G_6G_7T G_8G_9C GT-3′ containing a single O^6-POB-dG residue at G_3, G_4, G_5, G_6, or G_7 (500 fmol) were incubated with human recombinant AGT (400 fmol) for 15 s, and O^6-POB-G adducts remaining in DNA were quantified by HPLC-ESI$^+$-MS/MS as shown in Figures 1 and 2.[31] The results were compiled from three different experiments (N = 9–14).

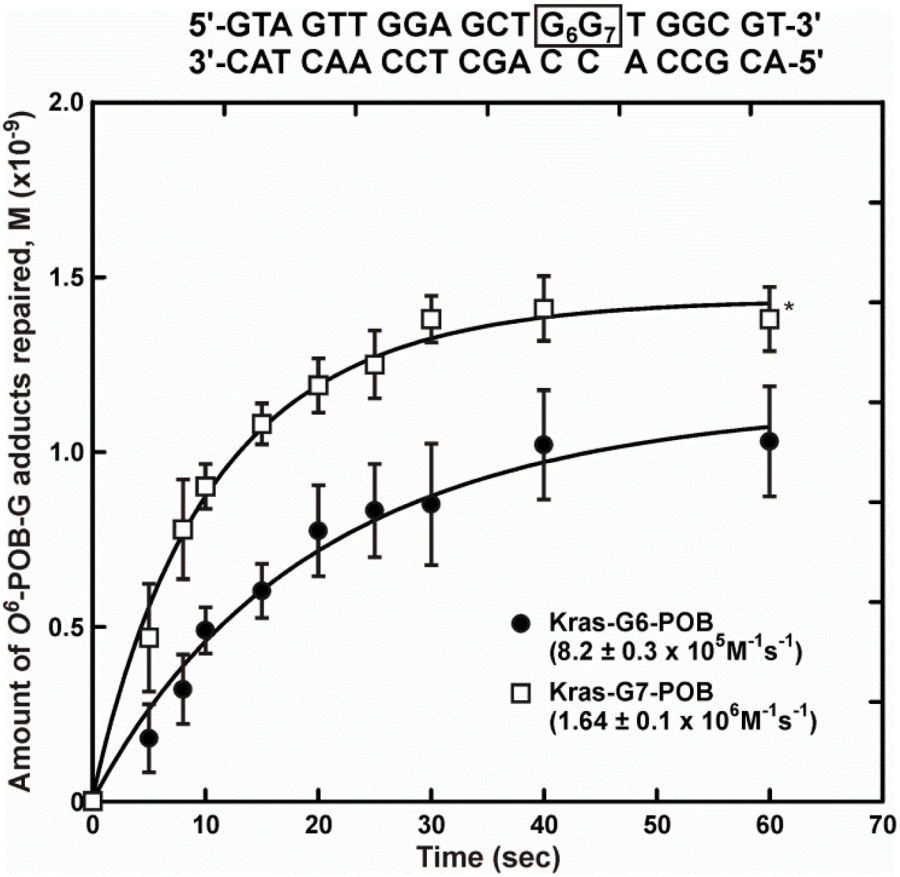

Figure 4.

Time course of AGT-mediated repair of O^6-POB-dG placed at the first (G_6) and the second position of *K-ras* codon 12 (G_7). O^6-POB-dG-containing duplexes (500 fmol) were incubated with recombinant human AGT protein (400 fmol) for increasing lengths of time (0–60 seconds), and the reactions were quenched with HCl. The unrepaired O^6-POB-G adducts remaining in DNA were quantified by isotope dilution HPLC-ESI$^+$-MS/MS.[31] The kinetic curves (N = 5, fit between 0–20 sec) represent the best fit to a second-order exponential equation that provides the rate of AGT-mediated dealkylation.

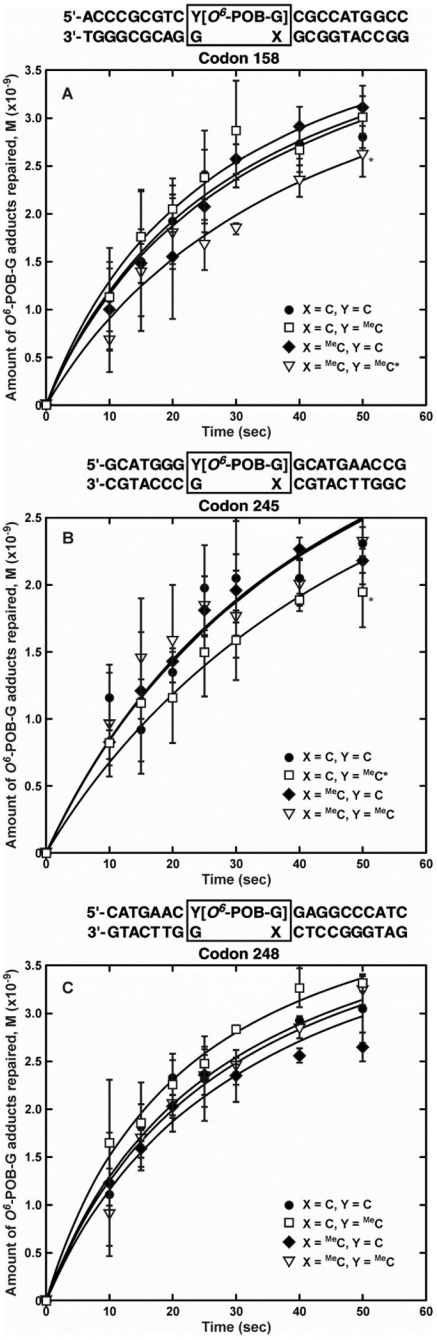

Figure 5.

Time course of AGT-mediated repair of O^6-POB-dG placed within synthetic duplexes representing unmethylated, hypomethylated, and fully methylated CG dinucleotides within *p53* codons 158, 245, 248. O^6-POB-dG-containing duplexes (500 fmol) were incubated with recombinant human AGT protein (400 fmol) for increasing lengths of time (0–50 seconds). The reactions were quenched with HCl, and the unrepaired O^6-POB-G adducts were quantified by isotope dilution HPLC-ESI$^+$-MS/MS.[31] The kinetic curves (N = 4) represent the best fit to a second-order exponential equation that provides the rate of AGT-mediated delakylation.

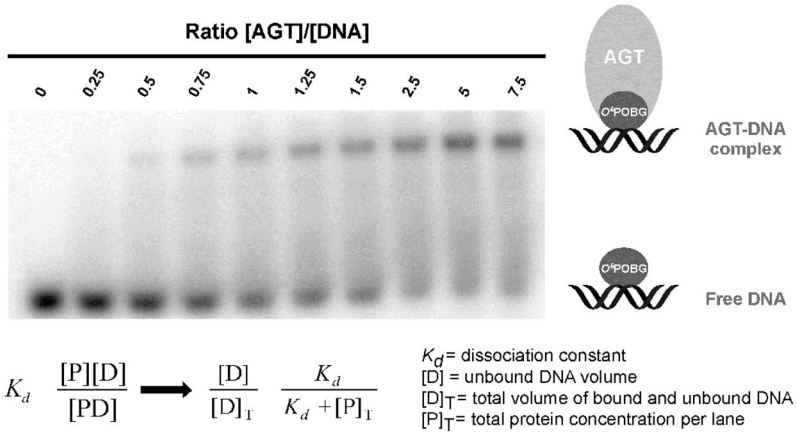

Figure 6.

Representative gel shift assay result used to determine the binding affinity of human AGT protein for O^6-POB-G-containing DNA duplexes. ^{32}P endlabeled DNA duplexes (5′-CATGAAC ^{Me}C [O^6-POB-G]GAGGCCCATC-3′ and the complementary strands (0.8 μM, in triplicate) were incubated with increasing amounts of C145A AGT protein, and the resulting AGT-DNA complexes were resolved by 10% non-denaturing PAGE.

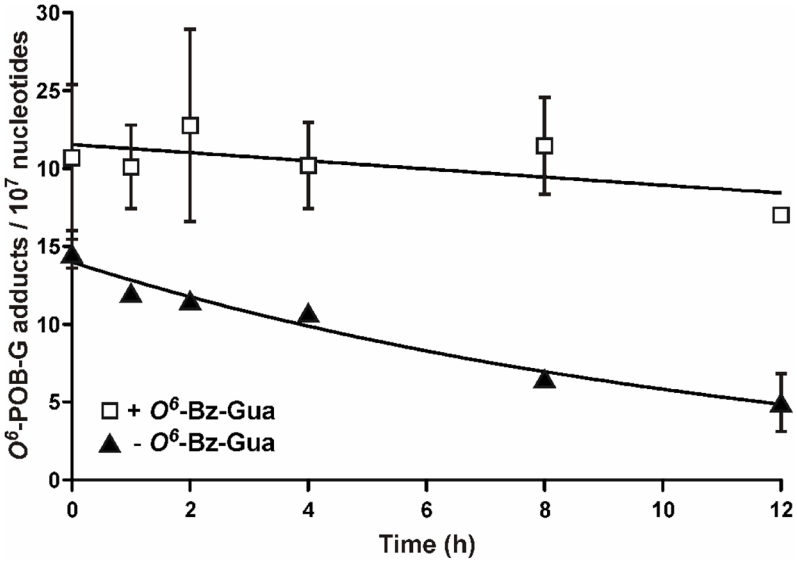

Figure 7.

Time dependent repair of O^6-POB-G adducts in normal human bronchial epithelial cells (HBEC). Cells in culture were treated with 150 μM NNKOAc for 1 hour in the presence or in the absence of AGT-inhibitor, O^6-Bz-G (10 μM). Following the removal of NNKOAc, cells were grown in normal media for 0 – 12 h (or media containing 5 μM O^6-Bz-G), and the kinetics of O^6-POB-G repair over time were determined by HPLC-ESI$^+$-MS/MS. N = 3 experiments were averaged for each experimental condition.

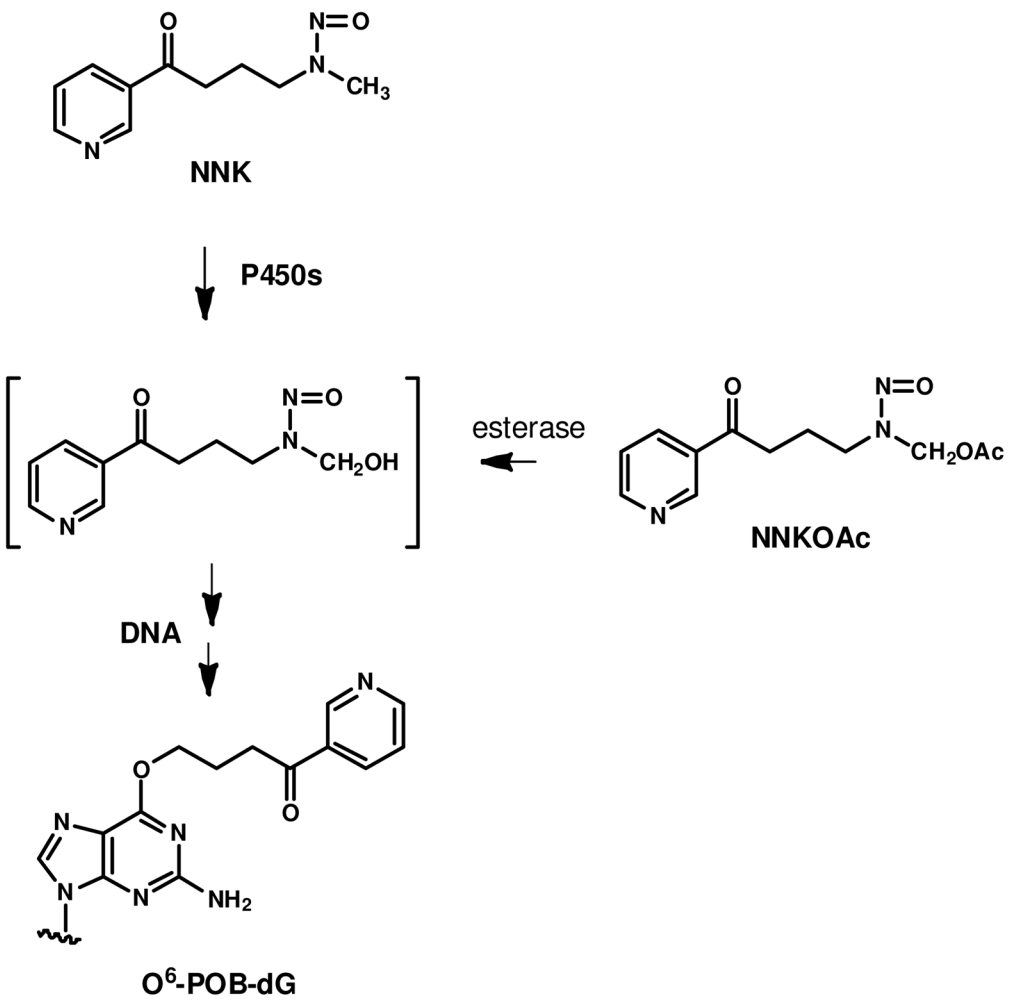

Scheme 1.
Metabolic activation of NNK and the formation of O^6-pyridyloxobutyl-dG adducts.

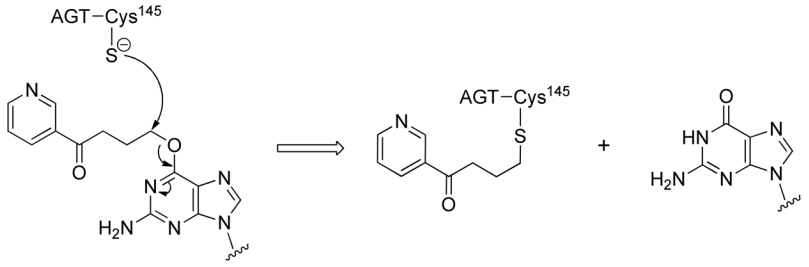

Scheme 2.
AGT repair of O^6-pyridyloxobutyl-dG adducts.

Table 1

Sequences and ESI$^-$ MS analysis results for synthetic DNA oligomers employed in this work.

Adduct location	Sequence	Calculated	Observed
		MW	
(+) *K-ras*- G3-POB	GTA GTT [O^6-POB-G]GA GCT GGT GGC GT	6407.3	6406.1
(+) *K-ras*- G4-POB	GTA GTT G[O^6-POB-G]A GCT GGT GGC GT	6407.3	6406.1
(+) *K-ras*- G5-POB	GTA GTT GGA [O^6-POB-G]CT GGT GGC GT	6407.3	6406.1
(+) *K-ras*- G6-POB	GTA GTT GGA GCT [O^6-POB-G]GT GGC GT	6407.3	6406.1
(+) *K-ras*- G7-POB	GTA GTT GGA GCT G[O^6-POB-G]T GGC GT	6407.3	6406.1
(−) *K-ras*-POB	ACG CCA CCA GCT CCA ACT AC	5975.9	5974.6
p53 codon 248	CATGAAC<u>C[O^6-POB-G]G</u>AGGCCCATC	5930.0	5930.4
	CATGAAC<u>^{Me}C[O^6-POB-G]</u>GAGGCCCATC	5944.0	5944.8
	GATGGGCCT <u>CCG</u> GTTCATG	5835.8	5835.6
	GATGGGCCT <u>C ^{Me}C G</u> GTTCATG	5849.9	5849.4
p53 codon 245	GCATGGGC[O^6-POB-G]GCATGAACCG	6476.3	6477.1
	GCATGGG^{Me}C[O^6-POB-G]GCATGAACCG	6490.3	6490.4
	CGGTTCAT <u>GCC</u> GCCCATGC	5740.8	5740.8
	CGGTTCAT <u>GC ^{Me}C</u> GCCCATGC	5754.8	5754.8
p53 codon 158	ACCCGCGTC<u>C[O^6-POB-G]C</u>GCCATGGCC	6026.0	6026.9
	ACCCGCGTC^{Me}C[O^6-POB-G]CGCCATGGCC	6040.1	6040.4
	GGCCATGGC <u>GCG</u> GACGCGGGT	6529.3	6529.4
	GGCCATGGC G^{Me}CG GACGCGGGT	6543.3	6543.2

Table 2

UV melting points of O^6-POB-G containing DNA duplexes.

Oligonucleotide ID	Sequence			T_m(°C)	
				Calculated[a,b]	Observed[c]
ds *p53* exon 5 codon 158, O^6-POB-G	ACCCGCGTCTGGGCGCAG	C[O^6-POB-G] / G C	CGCCATGGCCGCGGTACCGG	75.0	74.89 ± 0.62
ds *p53* exon 5 codon 158, 5′-^{Me}C, O^6-POB-G	ACCCGCGTCTGGGCGCAG	^{Me}C[O^6-POB-G] / G C	CGCCATGGCCGCGGTACCGG		75.31 ± 1.37
ds *p53* exon 5 codon 158, BP-^{Me}C, O^6-POB-G	ACCCGCGTCTGGGCGCAG	C[O^6-POB-G] / G ^{Me}C	CGCCATGGCCGCGGTACCGG		74.86 ± 0.78
ds *p53* exon 5 codon 158, Both-^{Me}C, O^6-POB-G	ACCCGCGTCTGGGCGCAG	^{Me}C[O^6-POB-G] / G ^{Me}C	CGCCATGGCCGCGGTACCGG		75.08 ± 1.15
ds *p53* exon 7 codon 245, O^6-POB-G	GCATGGGCGTACCC	C[O^6-POB-G] / G C	GCATGAACCGCGTACTTGGC	66.0	64.71 ± 0.93
ds *p53* exon 7 codon 245, 5′-^{Me}C, O^6-POB-G	GCATGGGCGTACCC	^{Me}C[O^6-POB-G] / G C	GCATGAACCGCGTACTTGGC		65.50 ± 1.28
ds *p53* exon 7 codon 245, BP-^{Me}C, O^6-POB-G	GCATGGGCGTACCC	C[O^6-POB-G] / G ^{Me}C	GCATGAACCGCGTACTTGGC		65.45 ± 1.22
ds *p53* exon 7 codon 245, Both- ^{Me}C, O^6-POB-G	GCATGGGCGTACCC	^{Me}C[O^6-POB-G] / G ^{Me}C	GCATGAACCGCGTACTTGGC		65.70 ± 0.70
ds *p53* exon 7 codon 248, O^6-POB-G	CATGAACGTACTTG	C[O^6-POB-G] / G C	GAGGCCCATCCTCCGGGTAG	64.0	61.01 ± 0.61
ds *p53* exon 7 codon 248, 5′-^{Me}C, O^6-POB-G	CATGAACGTACTTG	^{Me}C[O^6-POB-G] / G C	GAGGCCCATCCTCCGGGTAG		62.96 ± 0.94

Biochemistry. Author manuscript; available in PMC 2014 June 11.

Oligonucleotide ID	Sequence			T_m(°C)	
				Calculated[a,b]	Observed[c]
ds *p53* exon 7 codon 248, BP-^{Me}C, O^6-POB-G	CATGAACGTACTTG	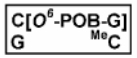	GAGGCCCATCCTCCGGGTAG		62.96 ± 0.61
ds *p53* exon 7 codon 248, Both- ^{Me}C, O^6-POB-G	CATGAACGTACTTG	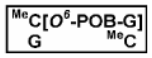	GAGGCCCATCCTCCGGGTAG		62.87 ± 1.17

[a] Calculated T_m does not include the presence of O^6-POB-G, instead a G was used <http://www.basic.northwestern.edu/biotools/oligocalc.html>

[b] 9.7 μM dsDNA with 66 mM salt (Na^+)

[c] T_m obtained from 4–6 hyperbolic curves

Table 3

Second order rate constants for AGT-mediated repair of O^6-POB-G adducts within unmethylated, hemi-methylated and fully methylated CG dinucleotides representing *p53* codons 248, 158, and 245.

Adduct Location	Sequence (5′ → 3′)			$k/10^6 (M^{-1} s^{-1})$
p53 exon 7 codon 248	CATGAACGTACTTG	C [O^6-Alk-G] G C	GAGGCCCATCCTCCGGGTAG	3.09 ± 0.16
	CATGAACGTACTTG	^{Me}C [O^6-Alk-G] G C	GAGGCCCATCCTCCGGGTAG	3.82 + 0.12
	CATGAACGTACTTG	C [O^6-Alk-G] G ^{Me}C	GAGGCCCATCCTCCGGGTAG	2.65 + 0.15
	CATGAACGTACTTG	^{Me}C [O^6-Alk-G] G ^{Me}C	GAGGCCCATCCTCCGGGTAG	2.94 ± 0.14
p53 exon 5 codon 158	ACCCGCGTCTGGGCGCAG	C [O^6-Alk-G] G C	CGCCATGGCCGCGGTACCGG	2.77 ± 0.13
	ACCCGCGTCTGGGCGCAG	^{Me}C [O^6-Alk-G] G C	CGCCATGGCCGCGGTACCGG	3.13 ± 0.2
	ACCCGCGTCTGGGCGCAG	C [O^6-Alk-G] G ^{Me}C	CGCCATGGCCGCGGTACCGG	2.65 + 0.16
	ACCCGCGTCTGGGCGCAG	^{Me}C [O^6-Alk-G] G ^{Me}C	CGCCATGGCCGCGGTACCGG	1.94 ± 0.11*
p53 exon 7 codon 245	GCATGGGCGTACC	C [O^6-Alk-G] G C	GCATGAACCGCGTACTTGGC	1.79 ± 0.14
	GCATGGGCGTACCC	^{Me}C [O^6-Alk-G] G C	GCATGAACCGCGTACTTGGC	1.37 ± 0.07*
	GCATGGGCGTACCC	C [O^6-Alk-G] G ^{Me}C	GCATGAACCGCGTACTTGGC	1.77 ± 0.08
	GCATGGGCGTACCC	^{Me}C [O^6-Alk-G] G ^{Me}C	GCATGAACCGCGTACTTGG	1.79 ± 0.12

Table 4

Dissociation constants for the interaction of O^6-POB-dG containing DNA duplexes with purified human C145A AGT protein.

Adduct Location	Sequence (5′ → 3′)			$K_d/10^{-6}$(M)
p53 exon 7 codon 248	CATGAACGTACTTG	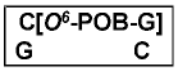	GAGGCCCATCCTCCGGGTAG	2.2 ± 0.4
	CATGAACGTACTTG	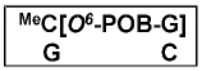	GGCCCATCCCGGGTAG	2.0 ± 0.2
	CATGAACGTACTTG		GAGGCCCATCCTCCGGGTAG	1.8 ± 0.3
	CATGAACGTACTTG	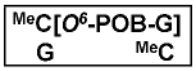	GAGGCCCATCCTCCGGGTAG	1.0 ± 0.1*
p53 exon 5 codon 158	ACCCGCGTCTGGGCGCAG	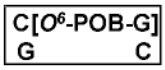	CGCCATGGCCGCGGTACCGG	2.3 ± 0.2
	ACCCGCGTCTGGGCGCAG	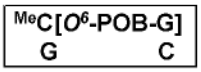	CGCCATGGCCGCGGTACCGG	4.8 ± 0.5*
p53 exon 7 codon 245	GCATGGGCGTACCC	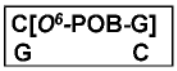	GCATGAACCGCGTACTTGGC	1.5 ± 0.3
	GCATGGGCGTACCC	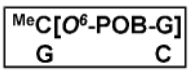	GCATGAACCGCGTACTTGGC	1.3 ± 0.1